Available online at www.sciencedirect.com
SciVerse ScienceDirect
Journal of Hydro-environment Research 8 (2014) 210–222
Journal of Hydro-environment Research
www.elsevier.com/locate/jher

Research paper

Development and application of 2-D mobile-bed model with bedrock river evolution mechanism

Chung-Ta Liao*, Keh-Chia Yeh, Ming-Wan Huang

Department of Civil Engineering, National Chiao Tung University, 1001 University Road, Hsinchu 30010, Taiwan

Received 27 August 2012; revised 20 February 2013; accepted 2 March 2013
Available online 15 March 2013

Abstract

Steep slope and severe bed change are the characteristics of mountain rivers. These characteristics often cause the bed armour layer flushed away, make the bedrock exposed, and then increase the channel incision. Most mobile-bed models of past few decades aimed at the sediment transport of alluvial channel. In this paper, a bedrock river evolution mechanism is proposed, and included in a 2-D mobile-bed model, called the explicit finite analytic model (EFA). The EFA model can consider both incision and deposition over the bedrock, by combining a new stream power type of bedrock erosion rate formula with the flow and sediment transport modules. An uplifted reach of Taan River, Taiwan, caused by the Chi–Chi earthquake occurred in 1999 is chosen as the study site. Rapid bedrock incision since the uplift provides a rare chance to explore its mechanism and evolution process. The field and numerical results show that the proposed model has the capability of simulating morphological changes for bedrock rivers.

Keywords: Bedrock river; Bedrock evolution; Erosion rate formula; Mobile-bed model; The Chi–Chi earthquake

1. Introduction

The evolution mechanism of bedrock river is different from that of alluvial river. Some researchers (e.g., Annandale, 1995; Sklar and Dietrich, 2004; Whipple, 2004; Carling, 2006; Chatanantavet and Parker, 2008, 2009; Lamb et al., 2008; Chatanantavet et al., 2010) studied the erosion mechanics of bedrock river during the past decades. Whipple (2004) stated that “bedrock channels lack a continuous cover of alluvial sediments, even at low flow, and exist only where transport capacity exceeds sediment flux over the long term.” Turowski et al. (2008) thought a bedrock channel cannot substantially widen, lower or shift its bed without eroding bedrock. These researches have contributed to the understanding of bedrock river evolution mechanism.

Through field investigation, there are three typical types of mechanisms responsible for the incision of bedrock: rock-block plucking, abrasion and cavitation. For rock-block plucking, it is a phenomenon which erodes and transports bedrock. The erosive power of flowing water is represented by its rate of energy dissipation for a variety of flow conditions (Annandale, 1995). Abrasion by bed-load or suspended-load is a ubiquitous and sometimes dominant erosion mechanism for fluvial incision into bedrock (Sklar and Dietrich, 2004). Cavitation on bedrock is caused by the impact of vapor bubbles generated from eddy or turbulence. It may contribute to the fluting and potholing of massive, unjointed rocks (Whipple et al., 2000).

In numerical bedrock model applications, Lai et al. (2011) proposed a two-dimensional mobile-bed model called SRH-2D that considered both hydraulic scour (plucking of rock fragments by fluid shear stress or different fluid pressure) and

* Corresponding author. Tel.: +886 3 5712121x54949; fax: +886 3 5724125.
E-mail addresses: zeromic@gmail.com (C.-T. Liao), kcyeh@mail.nctu.edu.tw (K.-C. Yeh).

1570-6443/$ - see front matter © 2013 International Association for Hydro-environment Engineering and Research, Asia Pacific Division. Published by Elsevier B.V. All rights reserved.
http://dx.doi.org/10.1016/j.jher.2013.03.001

abrasive scour (interaction between rock and moving sediment particles) of bedrock erosion mechanisms. SRH-2D model was applied to simulate the bed evolution downstream of Chi–Chi weir in Choushui River, Taiwan. Yeh et al. (2008) also presented a bedrock model which modified the abrasion model of Sklar and Dietrich (2004) to simulate the Chi–Chi weir case using the CCHE2D model. Although both the models had carried out in simulating the morphological changes of bedrock rivers, the CCHE2D had some limitations in simulating the case of composite bedrock materials, and more bedrock model parameters used in SRH-2D sometimes led to increase complexity in model calibration.

Steep slope and severe bed change during floods are the common characteristics in Taiwan's rivers. These characteristics often cause the bed armour layer flushed away when upstream sediment supply is insufficient. It makes the soft bedrock exposed, increase the channel incision, and endanger the safety of protection works along the river. Mobile-bed models of past few decades often aimed at the simulation of fluvial channel's sediment transport and bed changes. However, the soft bedrock river incision processes are different from those of alluvial rivers. To accurately analyze the bedrock river evolution, the development of 2-D mobile-bed model with bedrock erosion mechanism is required.

The purpose of this study is to develop a 2-D mobile-bed model with bedrock erosion mechanism for natural rivers. Meanwhile, the model's framework, bedrock erosion mechanism and its limitations are discussed in this paper. An uplifted reach of Taan River, Taiwan, caused by the Chi–Chi earthquake occurred in 1999 is chosen as the study site. A new stream power type of bedrock erosion rate formula based on the in-situ data is proposed and applied to simulate the rapid incision process. An equilibrium sediment concentration profile (van Rijn, 1984) is also considered in the model to compute the sediment exchange rate over the riverbed. All required topographic data, physical properties and parameters associated with alluvial and bedrock riverbeds adopted in the model were surveyed and measured from 1998 to 2009.

2. EFA model

A two-dimensional mobile-bed model, called explicit finite analytic model (EFA) is adopted in this study. The details of EFA model can be referred to Hsu et al. (2000) and Lin et al. (2006). Followings are the brief descriptions of flow and sediment transport modules.

2.1. Flow module

The continuity and momentum equations for water flow in the two-dimensional depth-averaged model can be expressed as:

$$\frac{\partial h}{\partial t}+\frac{\partial(\overline{u}h)}{\partial x}+\frac{\partial(\overline{v}h)}{\partial y}=0 \tag{1}$$

$$\frac{\partial\overline{u}}{\partial t}+\overline{u}\frac{\partial\overline{u}}{\partial x}+\overline{v}\frac{\partial\overline{u}}{\partial y}+\frac{1}{h}\frac{\partial}{\partial x}\left[\int_{z_b}^{z_s}u^2dz\right]+\frac{1}{h}\frac{\partial}{\partial y}\left[\int_{z_b}^{z_s}uvdz\right]=-g\frac{\partial(z_b+h)}{\partial x}+\frac{\nu_t}{h}\int_{z_b}^{z_s}\left(\frac{\partial^2 u}{\partial x^2}+\frac{\partial^2 u}{\partial y^2}\right)dz-g\frac{\overline{u}\sqrt{\overline{u}^2+\overline{v}^2}}{hC_h^2} \tag{2}$$

$$\frac{\partial\overline{v}}{\partial t}+\overline{u}\frac{\partial\overline{v}}{\partial x}+\overline{v}\frac{\partial\overline{v}}{\partial y}+\frac{1}{h}\frac{\partial}{\partial x}\left[\int_{z_b}^{z_s}uvdz\right]+\frac{1}{h}\frac{\partial}{\partial y}\left[\int_{z_b}^{z_s}v^2dz\right]=-g\frac{\partial(z_b+h)}{\partial y}+\frac{\nu_t}{h}\int_{z_b}^{z_s}\left(\frac{\partial^2 v}{\partial x^2}+\frac{\partial^2 v}{\partial y^2}\right)dz-g\frac{\overline{v}\sqrt{\overline{u}^2+\overline{v}^2}}{hC_h^2} \tag{3}$$

where t = time; x, y, and z = Cartesian coordinates; u and v = flow velocities in the x- and y-directions; $\overline{u}$ and $\overline{v}$ = depth-averaged velocities; h = water depth; z_b = bed elevation; z_s = water surface elevation; C_h = Chezy coefficient; g = gravitational acceleration; and ν_t = eddy viscosity.

The EFA method finds the local analytic solution on each nodal point within a local element. Regarding the momentum equations, nonlinear feature of the convective terms makes it impossible to obtain an analytic solution for the entire flow field. However, the nonlinear convection terms can locally be linearized by simply substituting the constant representative velocities for the convective velocities, called the characteristic velocities, so that the local analytic solutions can be obtained on the individual discretized nodal points. Although the convective velocities vary with space and time, the constant characteristic velocities could be used to represent the average convective feature in a local cell element during a small time step. The remaining problem is to determine the appropriate characteristic velocities for each local cell element. In EFA model, iteration procedure is adopted to update the solved variables, the source terms, and the characteristic velocities. Note that the newly calculated velocities during iterations are assumed to be the characteristic velocities. Additionally, iteration couples the momentum and continuity equations for flow and stops when the solution converges during each time step.

2.2. Sediment transport module

The mass-conservation equation for each particle size, k, of suspended sediment can be expressed as:

$$\left[\frac{D\overline{c}}{Dt}=\frac{\partial\overline{c}}{\partial t}+\left(\overline{V}\cdot\nabla\right)\overline{c}=\frac{S}{(h-\delta_a)}\right]_k \quad k=1,2,\ldots,\mathrm{TK} \tag{4}$$

where $\overline{c}$ is an averaged concentration evaluated from the reference level to the free surface; $\overline{v}$ = transport velocity of suspended sediment particles, assumed same as the flow velocity, in longitudinal x-direction and transverse y-direction, respectively; S = sediment exchange rate at the reference level; δ_a = reference level, which is assumed to be equal to half the bed-form height, or the equivalent roughness height;

subscript k is the sediment particle index; and TK = number of particle size classes. Mass balance of sediment in the active-layer can be expressed as:

$$\rho_s\left(1-p\right)\frac{\partial(\beta_k E_m)}{\partial t}+\left[\nabla\cdot\vec{q}_b+\rho_s\left(S-S_f\right)\right]_k=0 \quad k=1,2,\ldots,\mathrm{TK} \tag{5}$$

where ρ_s = density of sediment particles; p = porosity of bed layer; β_k = particle size fraction in the active-layer; E_m = active-layer thickness, which is just below the bed surface; $\vec{q}_b$ = bed-load flux; S_f = sediment exchange rate at the active-layer floor. Mass balance for bed materials is governed by

$$\rho_s(1-p)\frac{\partial z_b}{\partial t}+\sum_{k=1}^{\mathrm{TK}}\left(\nabla\cdot\vec{q}_b+\rho_s S\right)_k=0 \tag{6}$$

The suspended sediment transport equation, Eq. (4), is a hyperbolic-type partial differential equation. The characteristics method is suitable for solving this type of equation, and therefore is adopted in the proposed model. Mass balance of sediment in the active-layer (Eq. (5)) and mass balance for bed materials (Eq. (6)) are discretized into algebraic equations by the control volume method. After abovementioned discretization procedures, the algebraic equations can be solved by the coupled scheme. At any computational point, there are 2 TK + 1 equations, and these nonlinear algebraic equations can be solved by the iterative Newton–Raphson method.

3. Bedrock module

3.1. Stream power bedrock erosion rate formula

An empirical relation between rate of energy dissipation of flowing water and erodibility of the material can represent the Hydraulic erodibility of bedrock river (Annandale, 1995). Incipient motion occurs when the erosive capacity of flow just exceeds the ability of bed material to resist removal, and signals the beginning of the scour process. Fig. 1 shows the erosion threshold for rock and other complex earth material developed by Annandale (2006). The rate of energy dissipation is considered to represent the relative magnitude of erosive power of flowing water. The erosion threshold equations can be expressed as:

$$P_c=0.48K_h^{0.44} \quad \text{for } K_h\le 0.1 \tag{7}$$

$$P_c=K_h^{0.75} \quad \text{for } K_h>0.1 \tag{8}$$

where P_c = critical stream power (kw/m^2); K_h = erodibility index of bed material.

The erodibility index, K_h, can be defined as:

$$K_h=M_s\cdot K_b\cdot K_d\cdot J_s \tag{9}$$

where M_s = mass strength number; K_b = block size number; K_d = discontinuity bond shear strength number; J_s = relative

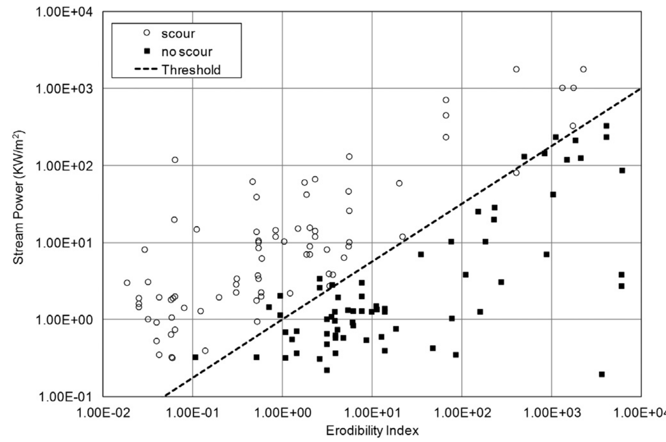

Fig. 1. Erosion threshold for rock and other complex earth material (redrawn from Annandale, 2006).

ground structure number. Erodibility index was originally developed by Kirsten (1982) to characterize the excavatability of earth materials. Annandale (2006) found that this index provides a good indicator of the relative ability of earth materials to resist the erosive capability of water. The erosion threshold method was based on an analysis of 137 field data of spillway performance collected by U.S. Department of Agriculture, observed at Bartlett Dam, Salt River Project, four South African dams, etc. When using these data in bedrock rivers, the erosion threshold is suggested to be re-modified or calibrated.

Generally, erosion rate for bedrock is a relation between flow velocity and rock properties. Erodibility index of bed material quantitatively represents the rock properties. Referring to Annandale's (2006) concept, this paper proposes an erosion rate formula and an erosion threshold for bedrock river using the field observations from 1998 to 2009 in Taan River (Liao et al., 2010; Huang et al., 2013).

Huang et al. (2013) pointed out two major observable forms of riverbed shaping processes in the uplifted reach of Taan River. The uniform incision over bedrock was activated soon after the armour layer being flushed away; subsequently, the inner gorge developed involving the actions of knickpoint migration and widening. The chronological longitudinal cross-sections along the main channel were analyzed in detail by Huang et al. (2013). The measured incision depth in the uplifted reach of Taan River from 2004 to 2005 (containing 17 locations along the channel) are used for the regression of the empirical formula in this study. The stream power, flow velocity, water depth and shear stress are calculated by hydraulic model under a fixed bed condition. The optimization by the nonlinear least-squares method is conducted to obtain the coefficients of the empirical formula. Based on the theorem mentioned above, the stream power type of bedrock erosion rate formula can be expressed as:

$$E=K_sU\left(\frac{P}{P_{\mathrm{cm}}}-1\right)^{0.2} \tag{10}$$

where E = erosion rate of bedrock riverbed (m/s); K_s = non-dimensional coefficient; U = depth-averaged velocity of flow (m/s); P = stream power of flow (kw/m^2), $P = \tau U$, τ = shear stress (N/m^2); P_{cm} = critical stream power in Taan River (kw/m^2), which can be described as:

$$P_{cm} = 0.12K_h^{0.15} \quad \text{for } 25 < K_h < 812 \tag{11}$$

Eqs. (10) and (11) are the first relation between rate of energy dissipation of flowing water and erodibility index of the bedrock material in Taiwan's River. This stream power bedrock erosion rate formula is included in the EFA model.

3.2. Bedrock evolution mechanism

3.2.1. Multiple bed layers

Field inspections indicate that the bedrock river is usually covered by a layer of coarse material on the floodplain or main channel. The bedrock erosion starts after the layer of bed material being flushed away. Bedrock river usually has a trend that upstream sediment supply is insufficient in the long term. In other words, it may result in deposition on the bedrock when the upstream sediment inflow increases or the morphology of the riverbed changes.

Bed materials above the riverbed could be divided into several layers since it usually varies on the vertical. Fig. 2 shows the modeling concept of multiple bed layers distributed in bedrock river. There are three types of bed material in the EFA model: alluvial bed, exposed bedrock and bedrock. The alluvial bed means the layer of fine or coarse material on the floodplains or riverbed. Sediment transport module is used to compute the suspended-load, bed-load, and bed changes. The exposed bedrock means the layer of rock that has been exposed due to the disappearance of armour layer above it. The erosion rate formula proposed in Eq. (10) is used to compute the bedrock degradation. Meanwhile, the sediment exchange rate will be considered to adjust whether the deposition occurs or not on the riverbed. The layer of bedrock means the layer under the alluvial bed or exposed bedrock. When the upper layers are flushed away, the under layer of bedrock would expose.

3.2.2. Sediment exchange rate

In EFA model, the equilibrium suspended sediment concentration profile, proposed by van Rijn (1984), can be expressed as:

$$c_e\left(z\right) = c_a\left[\frac{\delta_a}{(h-\delta_a)}\right]^{\phi} e^{-4\phi(z/h-0.5)} \quad \text{for } \frac{z}{h} \geq 0.5 \tag{12}$$

$$c_e(z) = c_a\left[\frac{\delta_a(h-z)}{z(h-\delta_a)}\right]^{\phi} \quad \text{for } \frac{z}{h} < 0.5 \tag{13}$$

where c_e is the equilibrium suspended sediment concentration; c_a is the reference concentration (van Rijn, 1984); $\phi = w_s/\beta_c \kappa u_*$, where w_s is the settling velocity of sediment, β_c is the ratio of sediment diffusion coefficient to fluid diffusion coefficient, κ is the von Karman coefficient, and u_* is the shear velocity at bed.

For the non-equilibrium suspended sediment concentration, additional flow-laden concentration at the reference level is defined as c_b. When c_b is larger than equilibrium reference concentration c_a, the flow is over-loaded; on the contrary, the flow is under-loaded. In EFA model, the form of flow-laden concentration profiles is assumed the same as equilibrium suspended sediment concentration profiles, which can be expressed as:

$$c(z) = c_b\left[\frac{\delta_a}{(h-\delta_a)}\right]^{\phi} e^{-4\phi(z/h-0.5)} \quad \text{for } \frac{z}{h} \geq 0.5 \tag{14}$$

$$c(z) = c_b\left[\frac{\delta_a(h-z)}{z(h-\delta_a)}\right]^{\phi} \quad \text{for } \frac{z}{h} < 0.5 \tag{15}$$

The concentration at the reference level, c_b, needs to be determined first (Lin et al., 2006). By adjusting the variable ϕ, the mass balance relation for the suspended load is satisfied:

$$\frac{1}{(h-\delta_a)} \int_{z=\delta_a}^{z=h} c(z)dz = \overline{c} \tag{16}$$

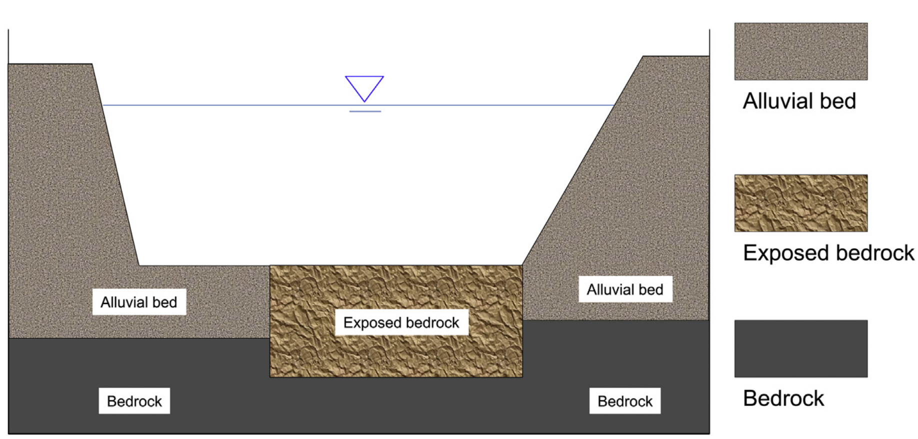

Fig. 2. Sketch of multiple bed layers in bedrock river.

where $\bar{c}$ is the depth-averaged concentration. The suspension parameter ϕ is the major factor to change the shape of concentration profile.

After knowing the equilibrium and flow-laden concentration profiles, one can tell the sediment-laden flow in either overloaded or under-loaded situation. Under non-equilibrium concentration condition, an active height can be defined as:

$$A_h = w_* \Delta t \tag{17}$$

where A_h = active height; w_* = velocity scale; Δt = time step in sediment transport module. The velocity scale is set to be either the settling velocity of sediment (w_s) for overloaded situation or the lifting velocity of sediment (w_l) for under-loaded situation. For bedrock riverbed, lifting velocity of sediment (w_l) is always zero. For alluvial riverbed, the lifting velocity of sediment defined here is as the initial velocity of saltation by Hu and Hui (1996):

$$\frac{w_l}{u_*} = \begin{cases} 3.2 - 4.5\log\Theta & \text{for } \Theta < 1.2 \\ 3.1 & \text{for } \Theta > 1.2 \end{cases} \tag{18}$$

where $\Theta = \tau_b / (\rho_s - \rho) g D$; τ_b = bed shear stress; ρ = density of flow; D = grain diameter.

The active height specifies a region above the reference level, over which the flow-laden concentration profile adjusts to its equilibrium profile for a given time step Δt. With this assumption, the sediment exchange rate within the given time step can be calculated by:

$$S = \frac{\int_{z=\delta_a}^{z=\delta_a + A_h} \left[c_e(z) - c(z)\right] dz}{\Delta t} \tag{19}$$

The flow-laden concentration profile is first calculated from previous time step, and S can be estimated by Eq. (19) in the present time step. The updated depth-averaged concentration and the corresponding flow-laden concentration profile then can be obtained through solving Eqs. (4) ∼ (6) simultaneously. According to the profile, the updated S can then be obtained. The iterations stop when the values of S have no difference during two consecutive iterations. Fig. 3 shows the definition sketch of sediment exchange rate about under-loaded and overloaded situation.

3.3. Model framework

The EFA model is de-coupled in solving the flow, sediment transport and bedrock modules. Sediment transport and bedrock modules usually use a larger time step than the flow module. In the beginning of computation, the initial condition is used for computing the steady state of flow field over the riverbed, and then the model will compute the unsteady flow for a given period of time. Based on the flow field, the sediment transport module can compute the sediment flux where the bed material is alluvial or bedrock. The bedrock module uses the stream power erosion rate formula to compute the bed degradation, and the sediment exchange rate adjusts whether the deposition occurs or not on the bedrock. The model is capable of setting different time steps for the flow, sediment transport and bedrock modules, respectively.

4. Model calibration and validation

4.1. Field site descriptions

4.1.1. Geological data

Taan River is 96 km in length, which is one of the major rivers in west-central Taiwan. Fig. 4 shows the Taan River watershed, the drainage area is about 758 km^2. Its upstream reach above the confluence at Baibufan is in the mountain area (bed elevation > 500 m), and the average bed slope is about 1/50. Downstream the confluence at Baibufan to the estuary, the average bed slope decreases from 1/76 to 1/90. The mean grain size of bed material sampled by 3rd River Management Office, Water Resources Agency, Taiwan, in 1993 was about 80 mm–190 mm.

In 1999, the Chi–Chi earthquake occurred with the earthquake center being located in central Taiwan. The tremor scale

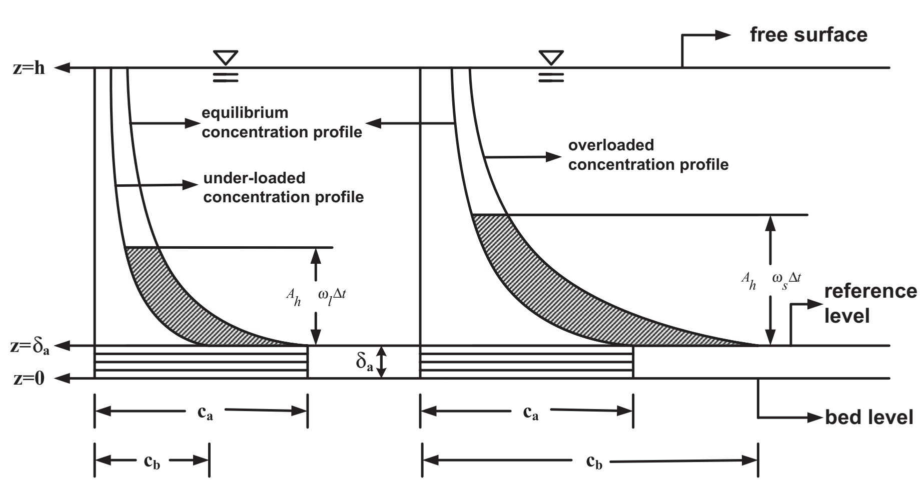

Fig. 3. Definition sketch of sediment exchange rate: (a) under-loaded situation; (b) overloaded situation.

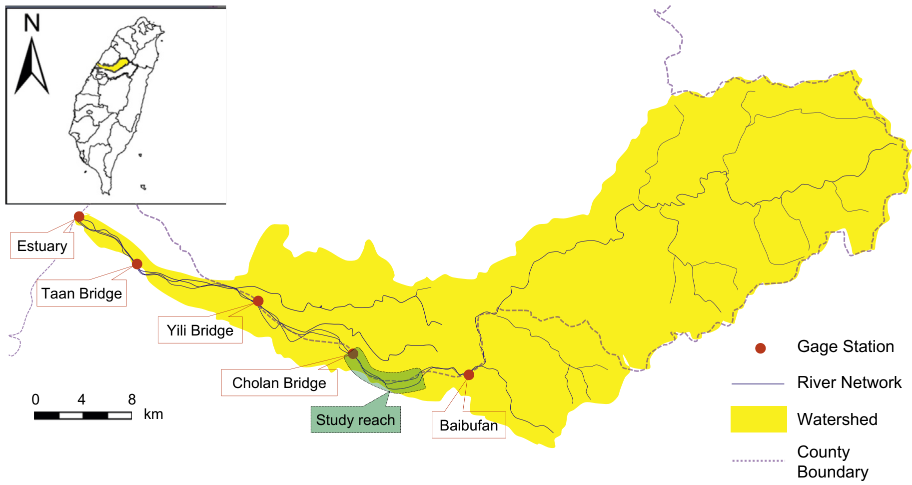

Fig. 4. Taan River watershed, Taiwan.

was 7.3 according to the Richter scale, and the focal depth was 8.0 km. A reach of Taan River was significantly uplifted (up to 10 m vertically) after the earthquake. Fig. 5 shows an aerial photo of the study reach from CS40 to CS51. The uplifted reach after the Chi–Chi earthquake is about 1.0 km long and 500 m wide, between CS44 to CS45. After the occurrence of the uplifting, the riverbed in this reach started to incise significantly in just a few years. In the field sights of channel from upstream to downstream, the upstream bed was covered by alluvial sediment, and the bedrock was almost exposed in the downstream where incised by the passage of bankfull discharges.

Fig. 6 shows the measured longitudinal bed elevation in the uplifted reach from 1998 to 2009. The maximum uplifted depth is about 10.0 m after the Chi–Chi earthquake, and the maximum erosion depth is over 18.0 m according to the measured data in 2009. The bed slope in 2009 is slightly steeper than that before the Chi–Chi earthquake. It shows the uplifted reach has been eroded toward its equilibrium state in ten years. The rapid bedrock incision data from 2000 to 2009 provide a real case to look into the mechanism and process of bedrock incision for sudden landform uplift caused by earthquake.

4.1.2. Hydrological data

In Taan River watershed, annual precipitation is between 1200 mm and 1800 mm and 80% of rainfall occurs in the summer. There is a gage station called Cholan, which is

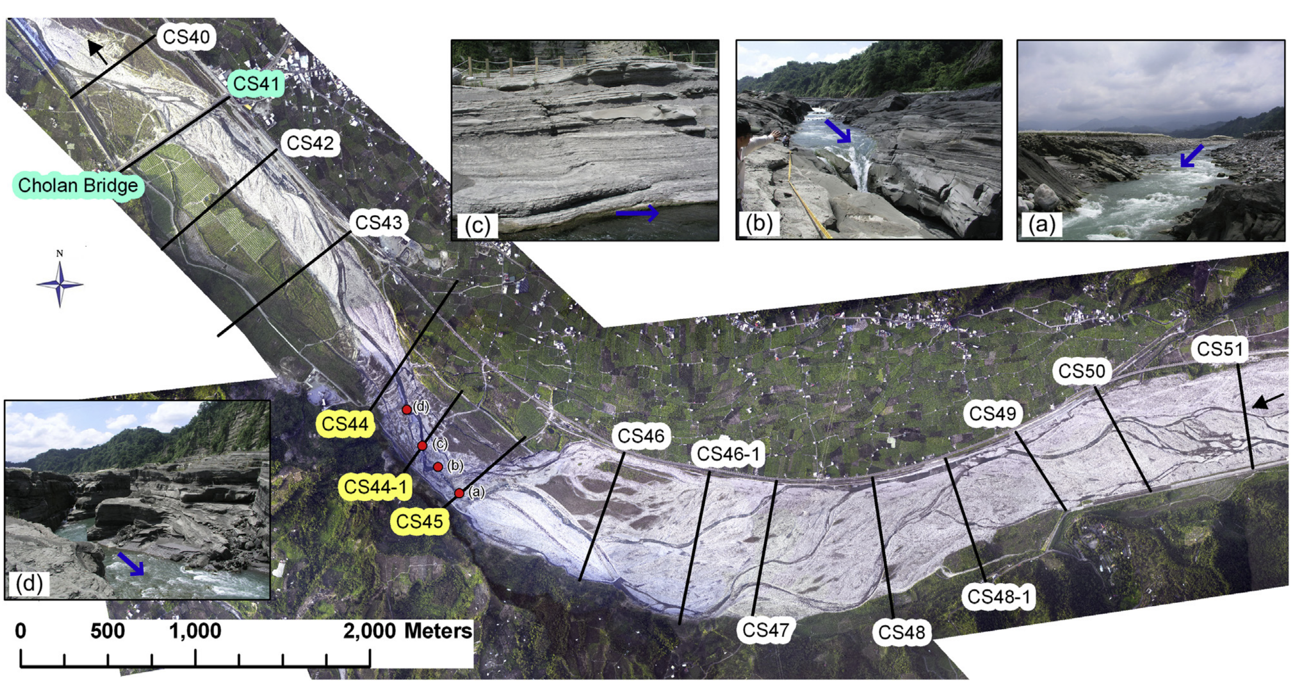

Fig. 5. Aerial photo of the study reach from CS40 to CS51. Field sights of uplifted reach, (a) alluvial bed in upstream; (b) the knickpoint; (c) bedrock channel in midstream; (d) severe bedrock incision in downstream (photo taken in 2008 and 2009 by the research team).

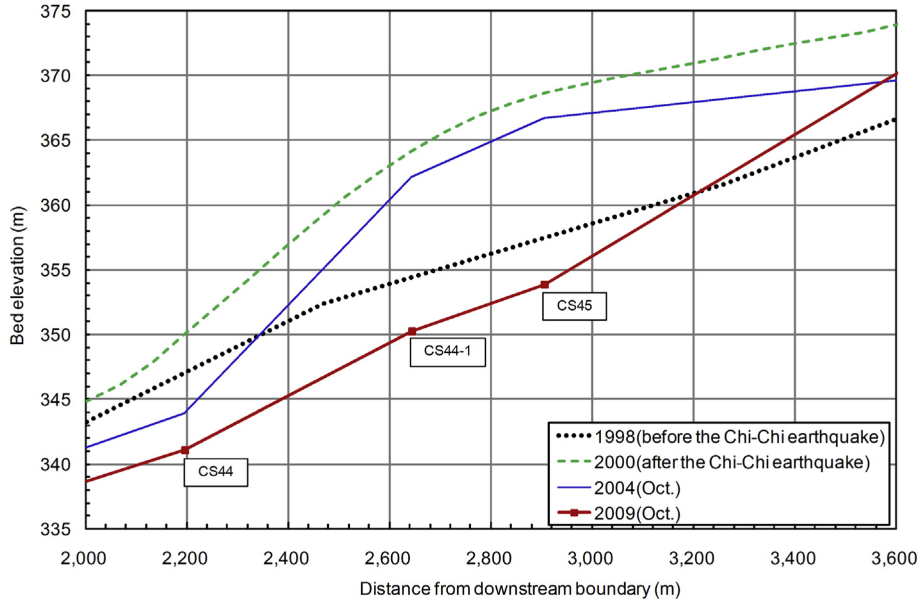

Fig. 6. Measured thalwegs in the uplifted reach of Taan River.

located at CS41 in the study reach. Based on the official managing and planning report, the 100-year return period discharge, Q_{100}, at Cholan gage station is 14,300 m^3/s, and the Q_2, Q_5 and Q_{10} is 2810 m^3/s, 5090 m^3/s, and 6910 m^3/s, respectively.

4.2. Initial and boundary conditions

The initial bed elevations of the computational mesh are interpolated and obtained using the cross-sectional data of 2000, and the data of 2004 and 2009 are used for the model calibration and validation, respectively. Fig. 7 shows the computational domain ranging from the upstream CS51 to the downstream CS40, which is about 7.0 km long, 550 m wide, and the average bed slope is larger than 1/90.

Fig. 7 shows the distribution of erodibility index (K_h) in 2000, which is used as the initial rock property for model calibration. The values of K_h surveyed and evaluated by the research team that ranges from 25 to 812. The bedrock exposed in the uplifted reach is the Pliocene Cholan Formation composed of sandstone, siltstone, mudstone, and shale in a monotonous alternating sequence. The Chi–Chi earthquake in

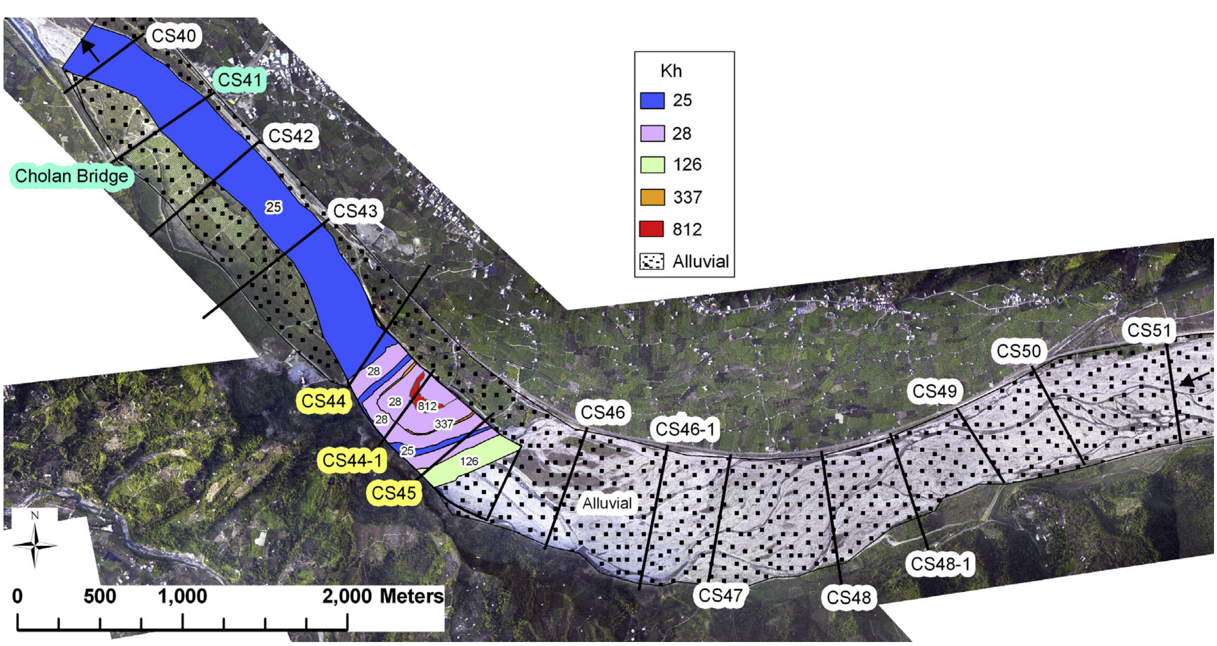

Fig. 7. Computational domain and the distribution of erodibility index (K_h) in 2000.

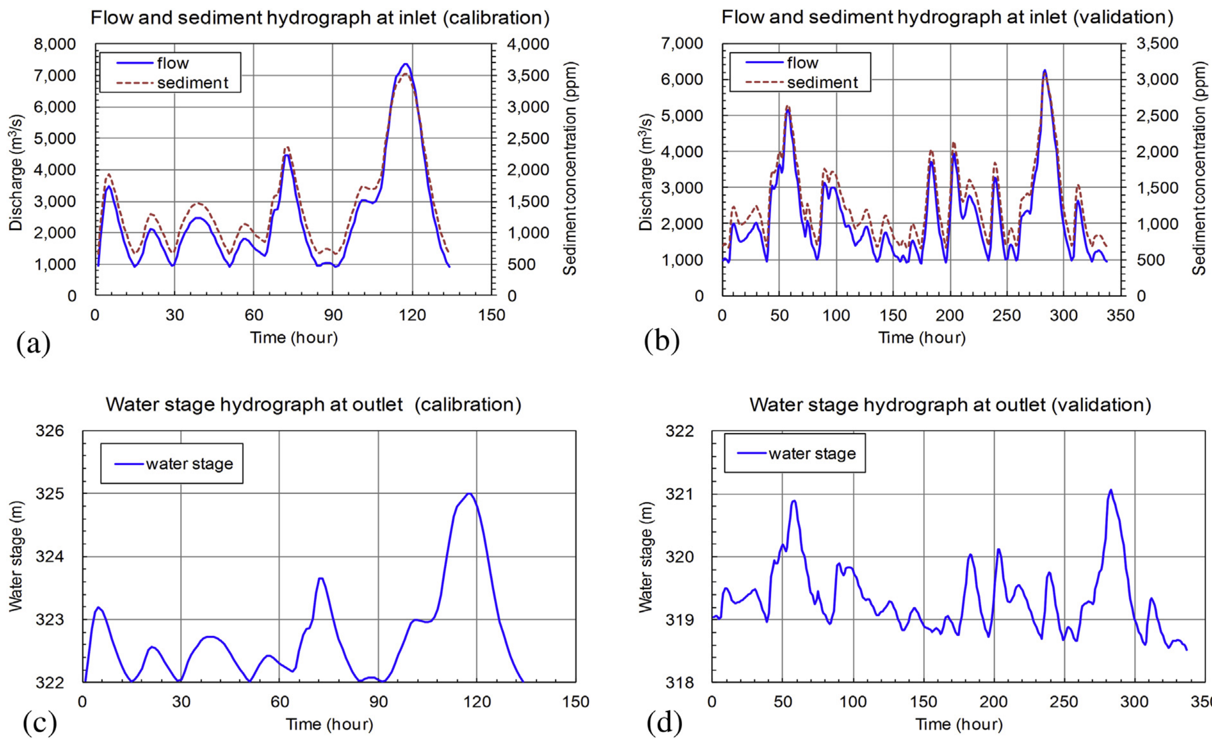

Fig. 8. Upstream and downstream boundary conditions for calibration and validation.

1999 uplifted the Tungshih anticline (Chen et al., 2007), which is the major geological structure in the study reach, and caused the young sediment rock more fractured and erodible.

Four types of rock layers are presented, including thin inter-layered sandstone and shale, massive sandstone, massive shale, and massive sandstone with occasional thin shale (Huang et al., 2013). In general, the unconfined compressive strength is under 10 MPa. Block size ranges from 10 cm to a few meters. Joint condition varies due to the influence of co-seismic uplift. The values of K_h are assigned according to the average value in each rock layers. The bed materials are almost alluvial sediment in the reach of CS46 to CS51. The main channel in the downstream reach (CS40 to CS45) is composed of exposed bedrock and the alluvial floodplains. The parameter of K_s in Eq. (10) was calibrated as 1.0e-6 to adjust the erosion rate of bedrock riverbed.

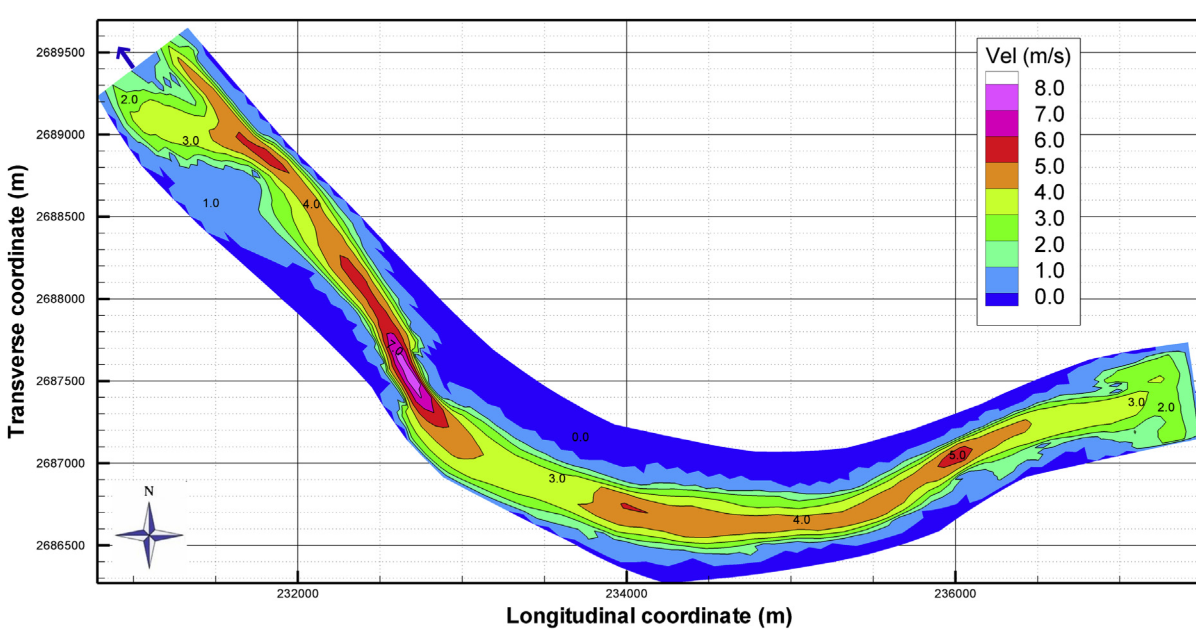

Fig. 9. Simulated velocity field at the initial discharge of 1041 m^3/s.

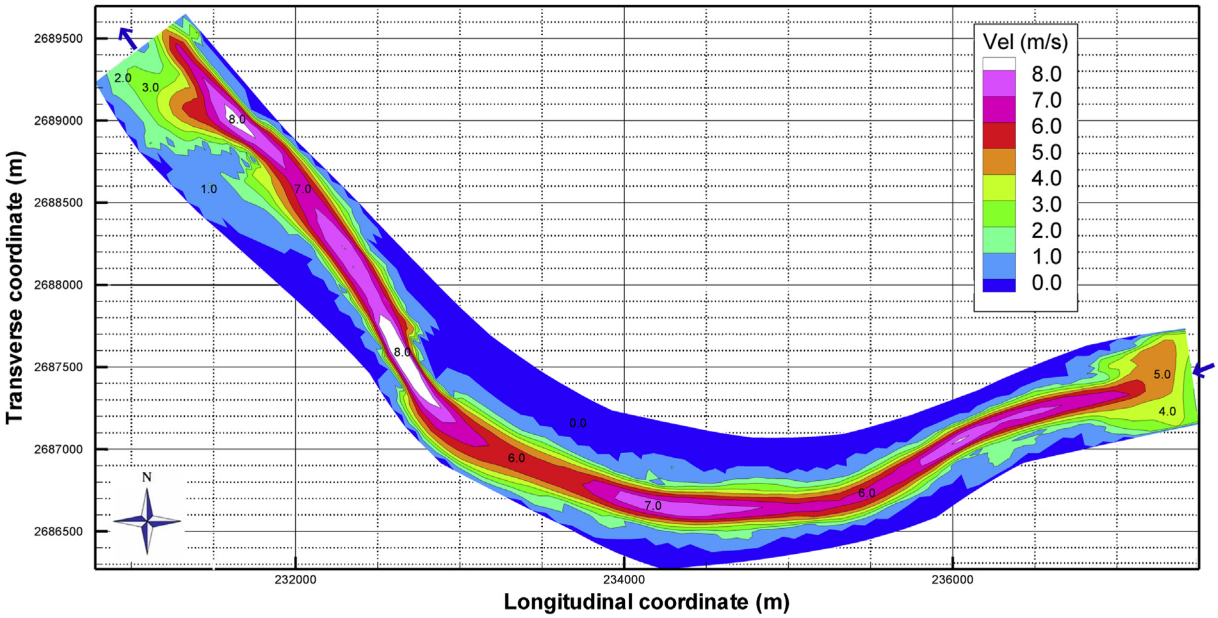

Fig. 10. Simulated velocity field at the peak discharge of 7367 m^3/s.

The bed materials obtained in 2000 are used as initial bed composition within the study reach. Three size classes ranging from 67.8 mm to 117.3 mm are selected to compute the associated sediment transport, and the Manning's coefficient is about 0.04. The thickness of active-layer, E_m, in Eq. (5) is related to the flow and sediment conditions as well as the bed change at the current time step. It is calibrated as 0.1 m through field data.

The EFA model is applied to simulate the morphological changes of the Taan River based on significant flood events during 2000–2009. Fig. 8(a) and 8(b) shows the flow and sediment hydrographs at the upstream and downstream boundary. The inflow hydrograph at the upstream is evaluated using the KW-GIUH model (Lee and Yen, 1997), and the sediment concentration is evaluated using the rating curve obtained from the measured suspended load data. The water stage hydrographs measured at Cholan gage station are used as the downstream boundary condition, shown as Fig. 8(c) and 8(d).

4.3. Model results and discussions

Figs. 9 and 10 show the simulated velocity fields at the initial and peak discharges, respectively, in the calibration case. When the inflow is low, the velocity ranged from 2.0 m/s to 4.0 m/s in the upstream reach. The maximum velocity is about 7.0 m/s near the maximum uplifted cross-section. When the peak discharge occurs, the velocity range from 6.0 m/s to

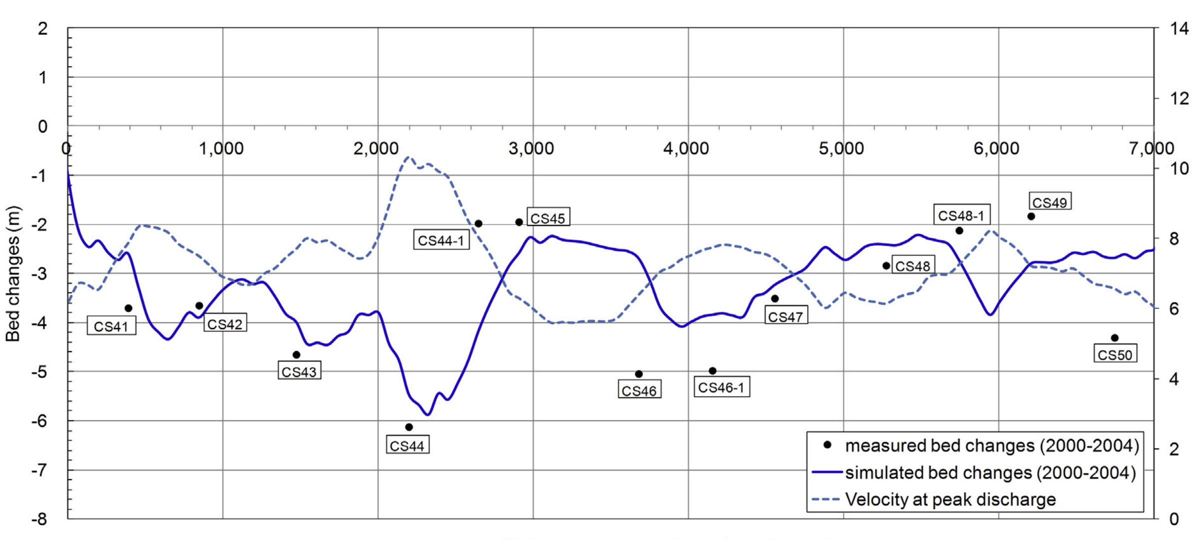

Fig. 11. Simulated and measured bed changes with velocity at peak discharge (calibration).

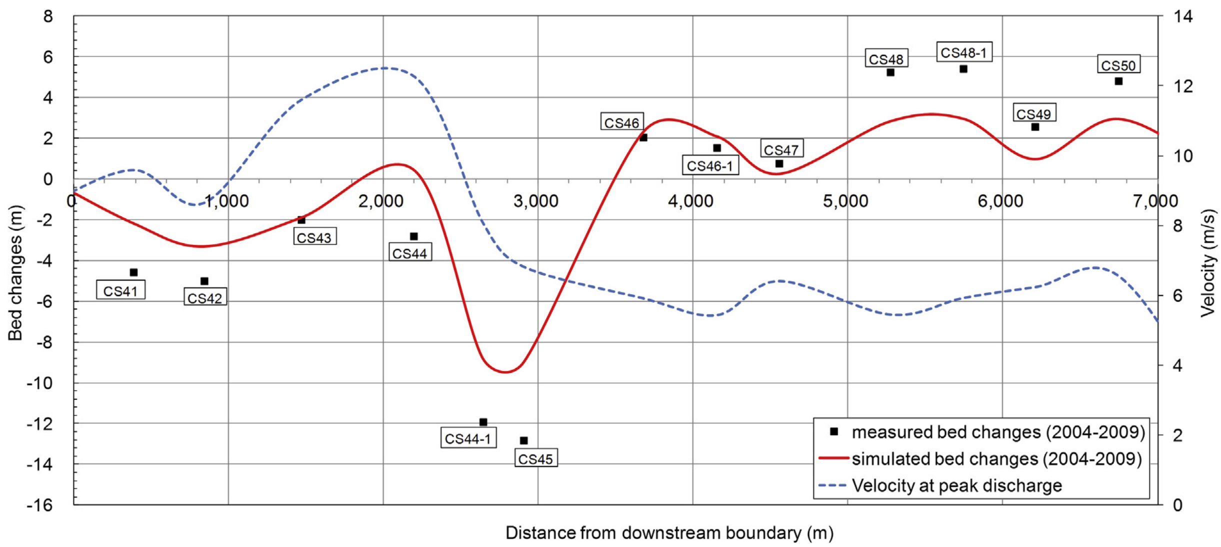

Fig. 12. Simulated and measured bed changes with velocity at peak discharge (validation).

8.0 m/s in the whole reach. As the inflow increases, the zone of high velocity in main channel has a trend of shifting toward upstream.

Figs. 11 and 12 show the bed changes and velocity along the study reach, the positive and negative values of bed changes relative to the initial bed elevation represents bed aggradation and degradation, respectively. It shows the maximum erosion depth from 2000 to 2004 was about 6 m. There is an almost uniform incision trend along the study reach in the calibration case, and the simulated bed changes agree well with the measured ones. Fig. 11 shows that the velocity corresponds to the severe bed degradation when the channel has a uniform incision trend.

In validation case, there is significant erosion near the uplifted reach. The maximum erosion depth is over 10.0 m according to the measured data in 2009. After the uniform incision occurs from 2000 to 2004, the bedrock riverbed starts to erode seriously near the uplifted reach from 2005 to 2009. The study reach has been eroded toward its equilibrium state in 2009 with the upstream reach having a slight deposition. The EFA model is capable of simulating the incision and deposition over the bedrock, as shown in the validation case.

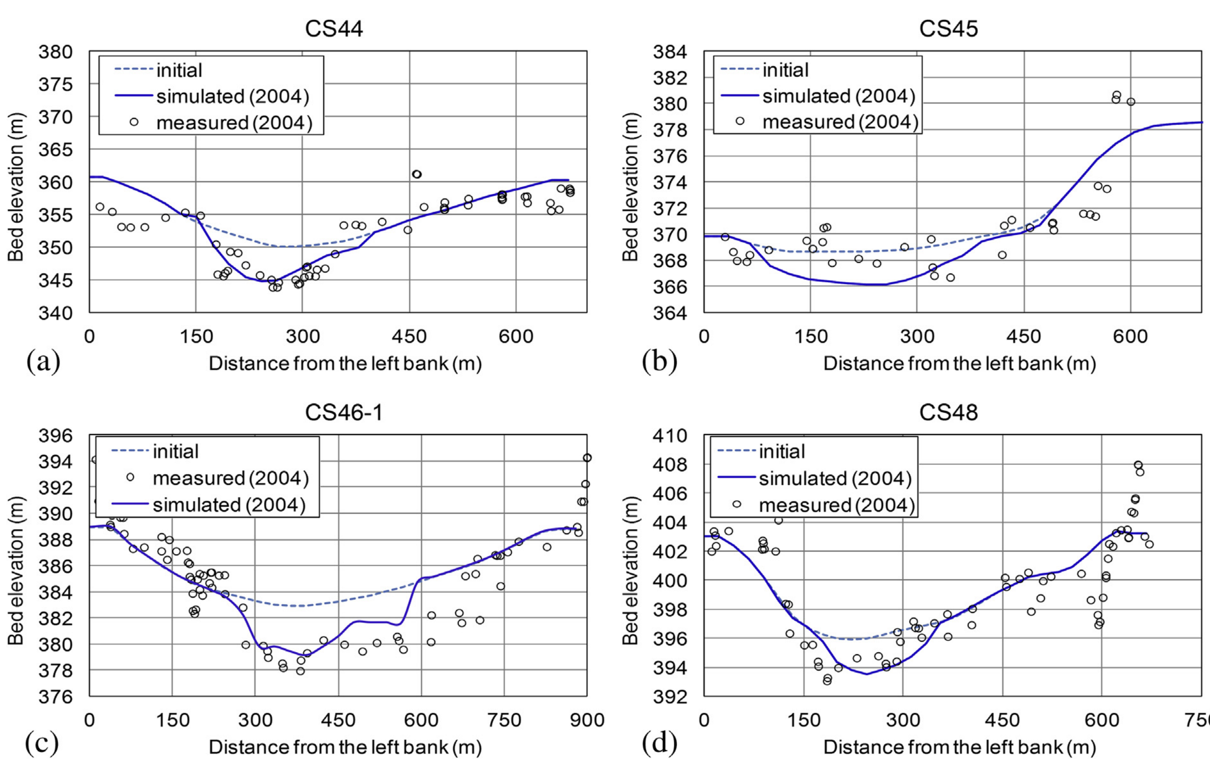

Fig. 13. Comparison of simulated and measured cross-sections (calibration).

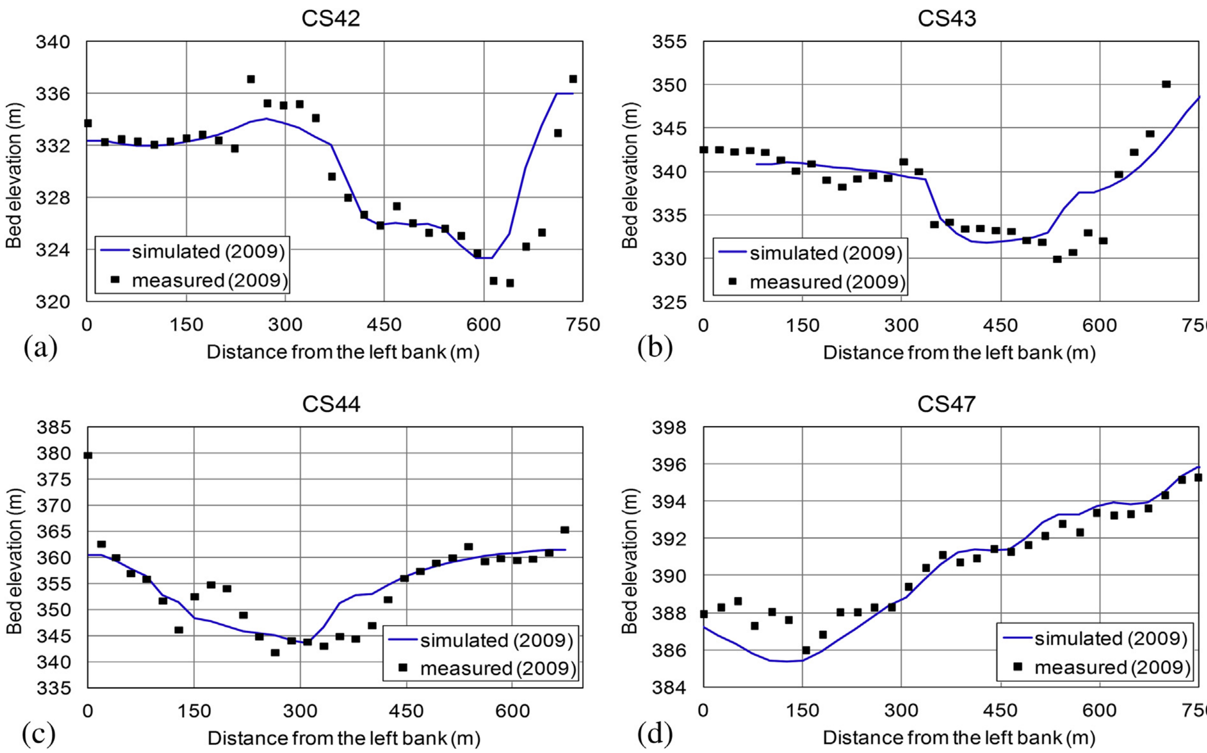

Fig. 14. Comparison of simulated and measured cross-sections (validation).

Figs. 13 and 14 show the comparison of simulated and measured cross-sectional data in the study reach. As shown in the calibration and validation cases, simulated bed changes in some cross-sections do not agree well with the measured data, especially near the bank region. This deviation may be due to the bank erosion and lateral migration mechanism of bedrock not being considered in the present model. Hence, the present bedrock module proposed herein has the limitation in simulating the lateral channel migration.

Fig. 15 compares the simulated bed profiles with the measured data after the significant floods occurred from 2000 to 2009. One can tell the bed elevation has severe changes after the Chi–Chi earthquake. From the observation of the bed slope in whole reach, the uplifted reach has been eroded toward its equilibrium state in ten years, and the downstream reach of CS44 is over-eroded compared with the bed before the Chi–Chi earthquake. According to the model performance in this study, the proposed model has the capability to simulate the bedrock erosion processes. Fig. 16 compares the simulated bed changes of thalwegs with measured ones in the calibration and validation cases. The data agree well and close to the diagonal line. It indicates that the model predicts the bed changes well on average.

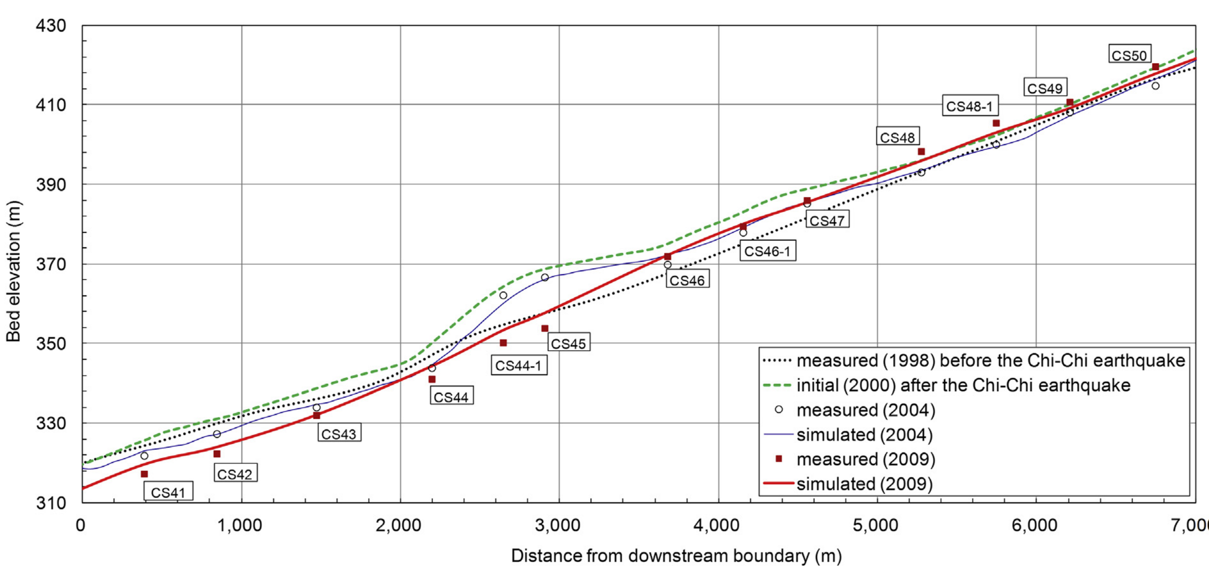

Fig. 15. Comparison of simulated and measured thalwegs.

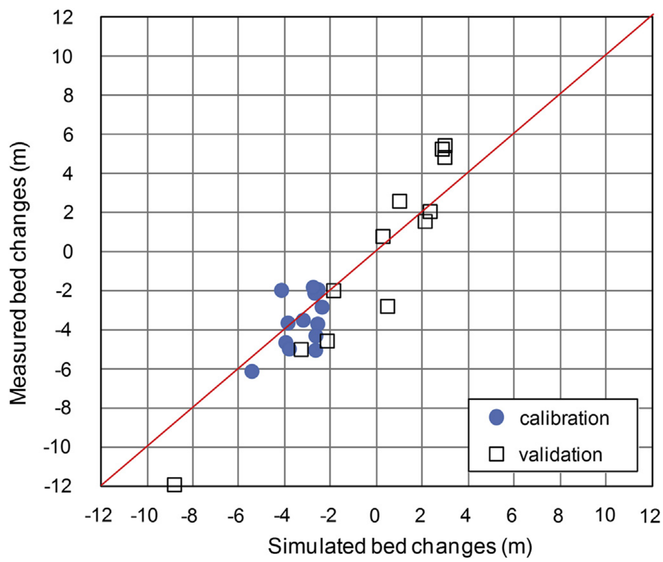

Fig. 16. Comparison of simulated and measured bed changes.

5. Conclusions

This paper presents a model (EFA) composed of the flow, sediment transport and bedrock modules. The sediment exchange rate and equilibrium concentration profile are considered in the model. Referring to the concept of Annandale (2006), a new erosion rate formula and an erosion threshold for bedrock are proposed using the field data obtained in Taan River, Taiwan. The EFA model has the capability of simulating the bedrock incision and deposition over the bedrock. Multiple bed layers and thickness include the bedrock, exposed bedrock and alluvial bed can be considered in the model. The simulated bed changes, thalwegs and cross-sectional profiles agree well with the measured data.

Through the field investigation and model simulation, it indicates that the velocity and critical stream power of flow could form a proper relation (e.g., Eq. (10)) of erosion threshold in bedrock rivers. In addition, the deviation at some cross-sections near the bank region of the study reach shows the bank erosion and lateral migration mechanism for bedrock rivers are needed in future to improve the accuracy of the simulation results.

Acknowledgments

The calculations were carried out on the IBM Cluster 1350 computer of the National Center for High-Performance Computing, Taiwan.

References

Annandale, G.W., 1995. Erodibility. Journal of hydraulic research 33 (4), 471—494. IAHR.

Annandale, G.W., 2006. Scour Technology, Mechanics and Engineering Practice. McGraw Hill, New York.

Carling, P.A., 2006. Editorial. The Hydrology and Geomorphology of Bedrock Rivers. Geomorphology 82, 1—3.

Chatanantavet, P., Parker, G., 2008. Experimental study of bedrock channel alleviation under varied sediment supply and hydraulic conditions. Water Resource Research 44, W12446. http://dx.doi.org/10.1029/2007WR006581.

Chatanantavet, P., Parker, G., 2009. Physical based modeling of bedrock incision by abrasion, plucking, and macroabrasion. Journal of Geophysical Research 114, F04018. http://dx.doi.org/10.1029/2008JF001044.

Chatanantavet, P., Lajeunesse, E., Parker, G., Malverti, Luce, Meunier, P., 2010. Physical based model of downstream fining in bedrock streams with lateral input. Water Resource Research 46, W02518. http://dx.doi.org/10.1029/2008WR007208.

Chen, Y.G., Lai, K.Y., Lee, Y.H., Suppe, J., Chen, W.S., Lin, Y.N.N., Wang, Y., Hung, J.H., Kuo, Y.T., 2007. Coseismic fold scarps and their kinematic behavior in the 1999 Chi-Chi earthquake Taiwan. Journal of Geophysical Research-Solid Earth 112, B03S02. http://dx.doi.org/10.1029/2006JB004388.

Hsu, C.T., Yeh, K.C., Yang, J.C., 2000. Depth-averaged 2-D curvilinear explicit finite analytic model for open channel flows. International Journal for Numerical Methods in Fluids 33, 175—202.

Hu, C., Hui, Y., 1996. Bed-load transport I: mechanical characteristics. Journal of hydraulic engineering, ASCE 122 (5), 245—254.

Huang, M.W., Pan, Y.W., Liao, J.J., 2013. A case of rapid rock riverbed incision in a coseismic uplift reach and its implications. Geomorphology 184, 98—110.

Kirsten, H.A.D., 1982. A Classification System for Excavation in Natural Materials. In: The Civil Engineer in South Africa, pp. 292—308.

Lamb, M.P., Dietrich, W.E., Sklar, L.S., 2008. A model for fluvial bedrock incision by impacting suspended and bed load sediment. Journal of Geophysical Research 113, F03025. http://dx.doi.org/10.1029/2007JF000915.

Lai, T.G., Greimann, B.P., Wu, K.W., 2011. Soft bedrock erosion modeling with a two-dimensional depth-averaged model. Journal of Hydraulic Engineering. ASCE 137 (8), 804—814.

Lee, K.T., Yen, B.C., 1997. Geomorphology and kinematic-wave-based hydrograph derivation. Journal of Hydraulic Engineering, ASCE 123 (1), 73—80.

Liao, J.J., Pan, Y.W., Yeh, K.C., Huang, M.W., Liao, C.T., 2010. Rapid Erosion Process of Soft Rock Riverbed — The Taan River as an Example (III). Water Resources Planning Institute, WRA, Taiwan (in Chinese).

Lin, E.T., Hsu, C.T., Yeh, K.C., 2006. Depth-integrated modeling for aggradating/degrading mobile channel I. model development. International Journal of Sediment Research 21 (4), 281—293.

Sklar, L.S., Dietrich, W.R., 2004. A mechanistic model for river incision into bedrock by saltating bed load. Water Resources Research 40, W06301. http://dx.doi.org/10.1029/2003WE002496.

Turowski, J.M., Hovius, N., Wilson, A., Horng, M.J., 2008. Hydraulic geometry, river sediment and the definition of bedrock channels. Geomorphology 99 (1), 26—38.

van Rijn, L.C., 1984. Sediment transport, Part II: suspended load transport. Journal of Hydraulic Engineering, ASCE 110 (11), 1613—1641.

Whipple, K.X., Hancock, G.S., Anderson, R.S., 2000. Mechanics and relative efficacy of plucking, abrasion, and cavitation. Geological Society of America Bulletin 112 (3), 490—503.

Whipple, K.X., 2004. Bedrock rivers and the geomorphology of active orogens. Annual Review of Earth and Planetary Science 32, 151—185.

Yeh, K.C., Wang, S.Y.Y., Jia, Y., Zhang, Y., Liao, C.T., 2008. Implement and Application Study of NCCHE's River Migration Models (II). Water Resources Planning Institute, WRA, Taiwan (in Chinese).

Mr. Liao, is a Ph.D. Candidate in Department of Civil Engineering, National Chiao Tung University, TAIWAN. He studied in numerical modeling of fluvial process, sediment transport, channel migration, and geomorphology. He is the co-developer of EFA model. In recent years, the modeling of bedrock incision process is carried out in EFA. Associated article has been presented and discussed in the 34th IAHR Biennial Congress (2011), Brisbane, Australia.

Dr. Yeh, is a Professor in Department of Civil Engineering, National Chiao Tung University, TAIWAN. He obtained his Ph.D. degree (1990) in the University of Iowa, Iowa, United States. He has published more than 20 papers in area of hydrology, numerical modeling, hydraulic engineering, sediment transport, and fluvial experiments. As a investigator, he has more than 25 years of working experience hosted the research projects of National Science Council and Water Resources Agency, Taiwan.

Mr. Huang, is a Ph.D. Candidate in Department of Civil Engineering, National Chiao Tung University, TAIWAN. He majored in geotechnical engineering, especially in engineering geology, rock mechanics, and geomorphology.